



Original Article

In situ calibration of observatory broadband echosounders

Egil Ona, Guosong Zhang *, Geir Pedersen , and Espen Johnsen

MEA, Institute of Marine Research, P. P. Box 1870, Bergen 5817, Norway

*Corresponding author: tel: 0047 95181677; e-mail: guosongzhang@hi.no.

Ona, E., Zhang, G., Pedersen, G., and Johnsen, E. *In situ* calibration of observatory broadband echosounders. – ICES Journal of Marine Science, 77: 2954–2959.

Received 19 June 2020; revised 2 September 2020; accepted 3 September 2020; advance access publication 19 November 2020.

Today, numerous scientific echosounders are used as continuously monitoring systems in ocean observatories. These echosounders are usually calibrated in shallow water, either in laboratory tanks or at random ocean docks before deployments. If the systems are used for quantitative measurements by the observatories, they should be calibrated at the operating depths to consider the environmental effects on the calibration parameters. In this article, a simple *in situ* calibration method is presented, which was recently applied to one of the nodes of the Norwegian Lofoten-Vesterålen ocean observatory, when the research vessel with dynamic positioning system suspended and moved the calibration sphere between the vessel and the transducer. The calibration results of a 70-kHz split-beam echosounder demonstrate that this method can be applied to the cabled observatories.

Keywords: calibration, echosounder, *in situ*, observatory

Introduction

Ocean observatories provide data of multiple oceanic variables for scientific researches (Favali and Beranzoli, 2006), and interests for real time data acquisitions have been realized by cabled ocean observatories that assist monitoring rapid changes, as well as long-term observations. Since the world's first regional cabled ocean observatory started operation in 2010 (Barnes *et al.*, 2010), it has become popular to apply this technology worldwide (Jacopo *et al.*, 2019), in which ocean instruments and sensors can be integrated into the cabled observatories, including inverted echosounders, hydrophones, cameras, and other sophisticated sensors. There are representative cabled observatories, such as the Norwegian Lofoten-Vesterålen (LoVe) observatory went into operation in 2013 (Godø *et al.*, 2014), the Ocean Observatories Initiative became operational in 2014 (Smith *et al.*, 2018), and the development of seafloor network stations in China (Yang *et al.*, 2020). The observatory instruments and sensors need to be calibrated to ensure the data quality, in which factory calibrations are usually applied pre-deployment and recalibrations are performed during redeployments (Smith *et al.*, 2019). The recalibration

intervals and methods may follow the guidelines of the manufactures. This article focuses on methods for calibrating inverted echosounders of cabled observatories.

Echosounder systems used for observing marine biological variations must be calibrated for quantitative measurements (Simmonds and MacLennan, 2005). In general, calibrations of a scientific echosounder should be performed within the range of environmental conditions (temperature and pressure) encountered during the measurements, preferably with the echosounder system installed on an instrument platform, for instance, a research vessel. The external environment may affect transducer performance of an echosounder, as the increased ambient pressure may affect the resonance frequency of a transducer and slightly change the transducer transmitting and receiving sensitivities (Ona, 1999; Andersen *et al.*, 2008; Andersen *et al.*, 2013; Haris *et al.*, 2018). An *in situ* calibration serves mainly three purposes: first, it calibrates the echosounder at an operating depth, and the combined effect of temperature and pressure on the transducer performance can be quantified; second, it can be used to monitor stability and performance of the echosounder at

regular intervals and help identify malfunctions; and third, it avoids retrieving the observatory platforms and expensive off-shore operations can be avoided.

Earlier studies on scientific echosounder transducers have mainly focused on the old types pressure resistant transducers (Dalen *et al.*, 2003; Patel and Ona, 2009), particularly the Simrad types ES38DD and ES120-7DD, which were constructed with arrays of ceramic elements moulded into the housings with front and backing material designed to withstand high pressure. It is shown that the performance of these transducers was affected by increasing pressure (Dalen *et al.*, 2003), in which the target strength (TS) measurements of the standard sphere show that TS increased with depth for the 38-kHz transducer, but decreased with depth for the 120-kHz transducer. For the TS variations at different depths, no hysteresis effect was observed on the Simrad DD type transducers, while the hysteresis of the EDO Western transducer was shown and investigated by Kloser (1996). Reanalysis of the measurements, with the old type split-beam transducer of Simrad ES120-7D used by Ryan *et al.* (2009), showed a more complex depth dependence in the report (Demer *et al.*, 2015).

Modern transducers used by the observatories are designed to withstand high hydrostatic pressures; e.g. the type Simrad ES70-7CD used by the LoVe observatory is designed to operate at a maximum depth of 1500 m. Although there are few publications on their performance variations at different operating depths, it is necessary to calibrate them at their operating depths in order to ensure unbiased measurements, and in addition to verify the calibration at a regular interval. A new and sophisticated echosounder calibration system could be used, particularly the deepwater calibration acoustic facility (DeCAF) (Haris *et al.*, 2018). However, the DeCAF requires to demount the whole echosounder system from host platform, and after calibration, the echosounder system will be mounted back to the host. This cannot be considered as a routine *in situ* method for cabled observatories. In 2005, Patel and Ona demonstrated *in situ* calibration using an underwater Remote Operated Vehicle (ROV) (Patel, 2006), but this method is limited by the expensive ROV operations.

In this article, we present a practical method for *in situ* calibrations of inverted echosounders of cabled observatories, using a research vessel with a dynamic positioning (DP) system. In May 2020, this method was applied to calibrate one echosounder of the LoVe observatory, when R/V Kronprins Haakon assisted. Based on the results, we suggest that this is an applicable and cost-efficient method for calibrating the echosounders of cabled observatories.

Calibration method

The LoVe observatory is a cabled ocean observatory operated by Institute of Marine Research (IMR). The initial observatory is now under expansion, it will consist of several observatory nodes, all of which are to be deployed in 2020. Figure 1 shows the location of first node (Node1) of the LoVe observatory, commenced in 2013 (Godø *et al.*, 2014), and it is operating at depth of 250 m. On the main lander of Node1, there is an inverted broadband echosounder (Simrad WBT mini) installed, supporting both continuous wave (CW) and linear frequency modulation (LFM) pulses. The calibration method was proposed for calibrating this echosounder on site.

In brief, a split-beam echosounder calibration involves a solid elastic sphere of known scattering properties placed within the acoustic beam of the transducer. When the sphere is moved throughout the acoustic beam while its TS is measured at numerous positions, beam parameters and axis gain can be extracted by a model fitting procedure (Ona, 1990; Ona and Barange, 1999; Demer *et al.*, 2015). The basic equations for split-beam TS measurements and volume backscattering are given (Ona *et al.*, 2009). Similar equations are used for a split-beam LFM TS measurements and volume backscattering, but all frequency-dependent parameters are now expressed as a function of frequency, f . System gain $G(f)$ and alongships and athwartships beamwidths are estimated following a similar procedure as for split-beam CW systems, reported by the echosounder reference manual (Simrad, 2020).

For the inverted echosounder, a surface vessel is required to assist suspending a calibration sphere during the measurements. Figure 2 shows the proposed *in situ* calibration method, which was applied to Node1 on 26 May 2020, when the researchers onboard monitored the calibration, storing and processing the data via remote control to the observatory server on shore. The Sea-Bird Scientific conductivity–temperature–depth (CTD) system was merely used as a ballast weight for keeping the calibration sphere stationary, but it could have been replaced by a large and acoustically resolvable stabilizing weight. If the CTD or a ballast weight has a strong backscatter accepted by the echosounder as a single target, it helps the initial positioning of the sphere inside the acoustic beam, when the operator onboard observes the echogram (the right panel). The acoustic footprint for positioning the calibration sphere was determined by observing the strong acoustic reflections from the Sea-Bird CTD (see Figure 2). The movement of the calibration sphere, particularly the 57.2-mm diameter tungsten carbide sphere, throughout the beam was achieved by R/V Kronprins Haakon using its DP system, DNV GL Class 1 (DNVGL, 2015). Once the beam had been located, the vessel locked to the exact position using its DP system and, thereafter, moved slowly and precisely to achieve the beam coverage required for calibration. The vessel's 70-kHz echosounder was in passive mode during the calibration to observe the background noise and avoid interference with the observatory echosounder transmitting every 2 s.

The selection of the relatively large calibration sphere was made for avoiding false detections of fish targets during the calibration. The sphere is specifically designed for rapid calibration of fishing vessels carrying multi-frequency echosounders at 18-, 38-, 70-, 120-, and 200-kHz frequencies (Slotte *et al.*, 2016). The sphere has a nominal CW (70 kHz) TS of -36 dB ref. 1 m² and is used in a similar manner as the larger tungsten carbide spheres for calibrating the Simrad ME70 and MS90 multibeam systems (Ona *et al.*, 2009).

Results

Figure 3 shows the movement of the vessel and the movement of the calibration sphere during the 44-min CW calibration. The vessel moved within a surface area of 24 m \times 18 m to achieve full coverage of the acoustic beam at 180 m range from the split-beam transducer (the top left panel of Figure 3). The top right panel shows the 514 detections of the calibration sphere, which are used for the CW calibration. As shown in the bottom panel of Figure 3, the vessel heave has a standard deviation of 0.37 m, and the range between the calibration sphere and the transducer does

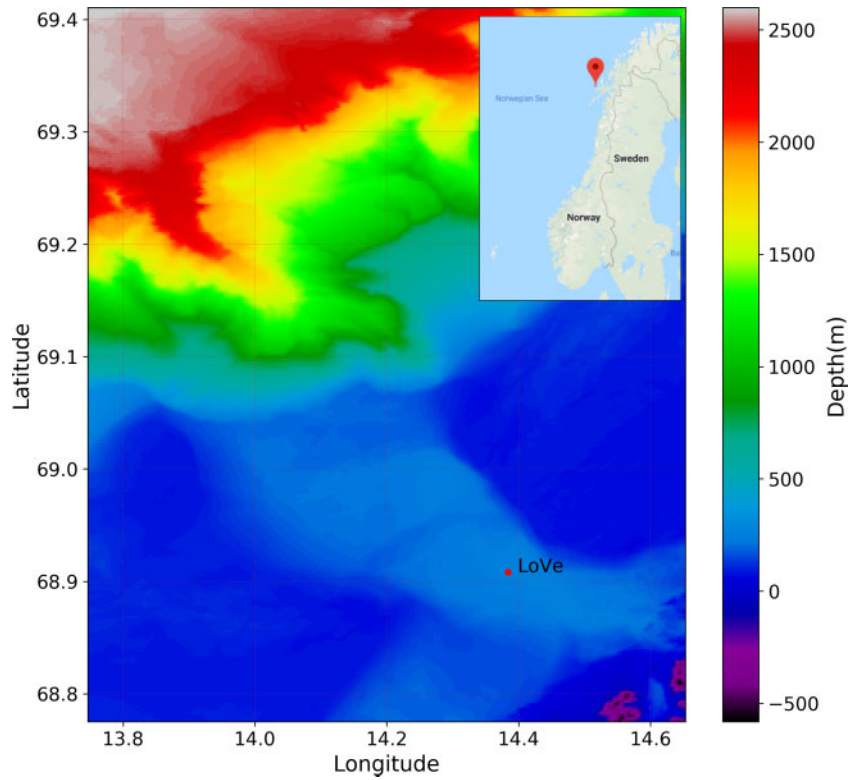


Figure 1. Node1 location of the LoVe observatory. Bathymetry data are provided courtesy of EMODnet (www.emodnet.eu).

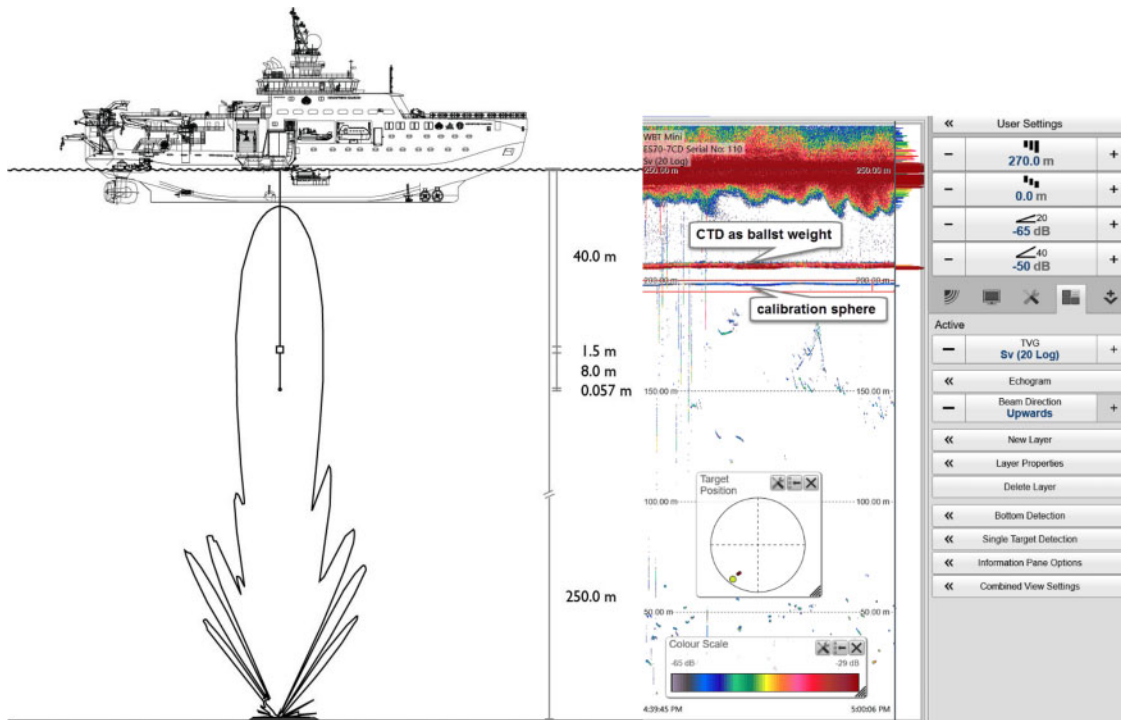


Figure 2. Illustration of the *in situ* calibration method applied to the LoVe observatory Node1 (the left panel) and a snapshot of the echogram observations from the observatory server (the right panel). The echosounder was deployed at the sea bottom, ~250 m below the sea surface. The R/V Kronprins Haakon assisted repositioning the calibration sphere within the acoustic beam. The sphere (57.2-mm diameter tungsten carbide with 6% cobalt binder) was netted using 0.6-mm diameter nylon line and was attached by 1.0-mm nylon line, 8 m below the Sea-Bird CTD system mounted inside a standard Carousel Water Sampler (1.5-m high), acting as a ballast suspended 40 m below the sea surface. The heave compensated winch lowered and kept the CTD system with the sphere from the starboard side of the vessel.

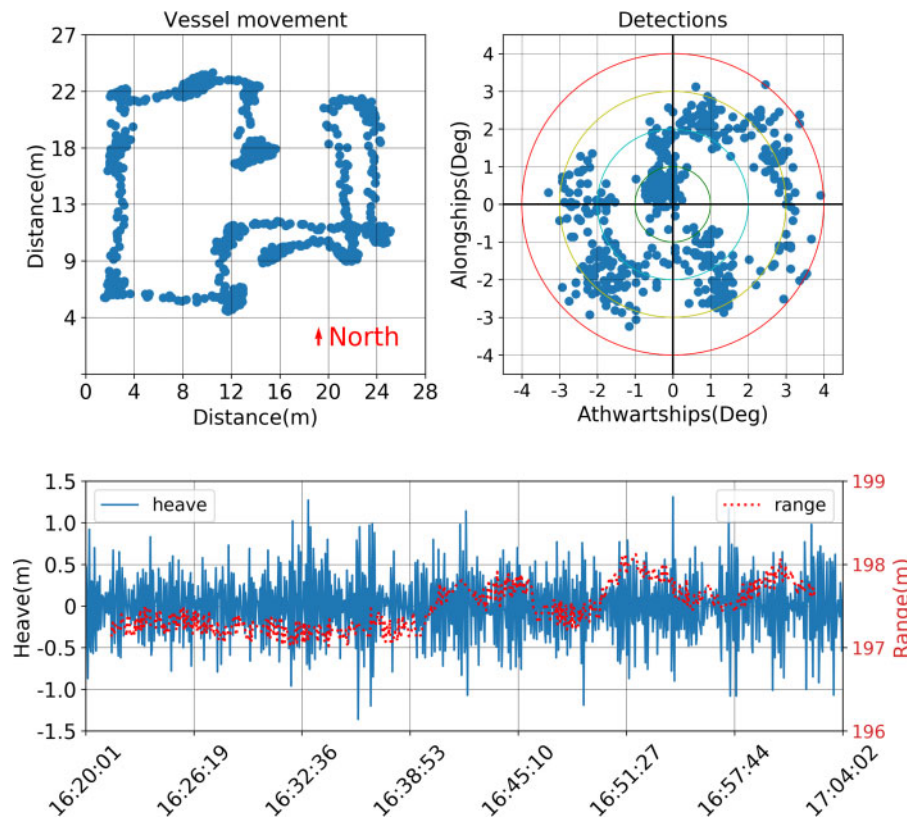


Figure 3. Movement of the vessel and the calibration sphere during the CW calibration. The top left panel shows the vessel positions within the surface area. The top right panel shows the target detections within the acoustic beam. The bottom panel shows the vessel heave and the range between the transducer and the calibration sphere. The heave was measured by the motion reference unit Kongsberg MRU 5. The mean wind speed was 14.8 m s^{-1} during this period, recorded by the weather station on the vessel. The R/V Kronprins Haakon kept fixed heading during this period.

not change very much because of using the heave compensated winch. The LFM calibration was performed in the same way as the CW calibration. After locating the beam of the Node1 transducer, in total it took $\sim 1.25 \text{ h}$ to complete both CW and LFM calibrations. Although the calibration programme of the Simrad EK80 software could be run in real time, the calibration results presented in this article were obtained after the survey by replaying the recorded data.

The calibration measurements were post-processed using Simrad EK80 software (version 1.12.4). Table 1 lists the prerequisite information for the calibrations, including the pulse information, and the sound speed, which is the average sound speed between the transducer and the calibration sphere. The signal-to-noise ratio in the layer used for calibration is between 18 and 20 dB, calculated by echo integration of the mean backscattering in a layer containing the calibration sphere and a neighbouring layer. Table 2 shows calibrated and nominal values from the CW measurements, in particular the TS transducer gain, half power beamwidths, and beam offset angles. The nominal values are measured just after production at the factory, in a fresh water tank at 20°C , by Simrad in 2013. The root mean square (RMS) error of the results is 0.3 dB.

Due to noise from power supply and other instruments on Node1, the echosounder used LFM pulse operating only from 67 to 87 kHz to avoid noise interference in the 45–67- and 87–90-kHz frequency bands. When using the Simrad echosounders in broadband mode, particularly using an LFM pulse, the reference

Table 1. Prerequisite information for calibrations.

Parameter	Information and value
Transducer	Simrad ES70-7CD (SN 110)
Transmission frequency (kHz)	70
Transmission power (W)	400
CW pulse duration (μs)	1 024
LFM pulse duration (μs)	2 048
LFM frequency band (kHz)	67–87
Tungsten carbide calibration sphere diameter (mm)	57.2
Equivalent beam angle (dB)	-20.7
Transducer angle sensitivity along alongships and athwartships	23
Absorption coefficient (dB km^{-1})	23.515
Sound speed (m s^{-1})	1 475

Table 2. CW calibration results.

Parameter	Calibrated	Nominal
TS transducer gain (dB)	28.86	27
Sa Correction (dB)	-0.16	0
Half power beamwidths along/athwartships ($^\circ$)	7.62/7.21	7.25/7.21
Offset along/athwartships ($^\circ$)	-0.08/-0.1	0/0

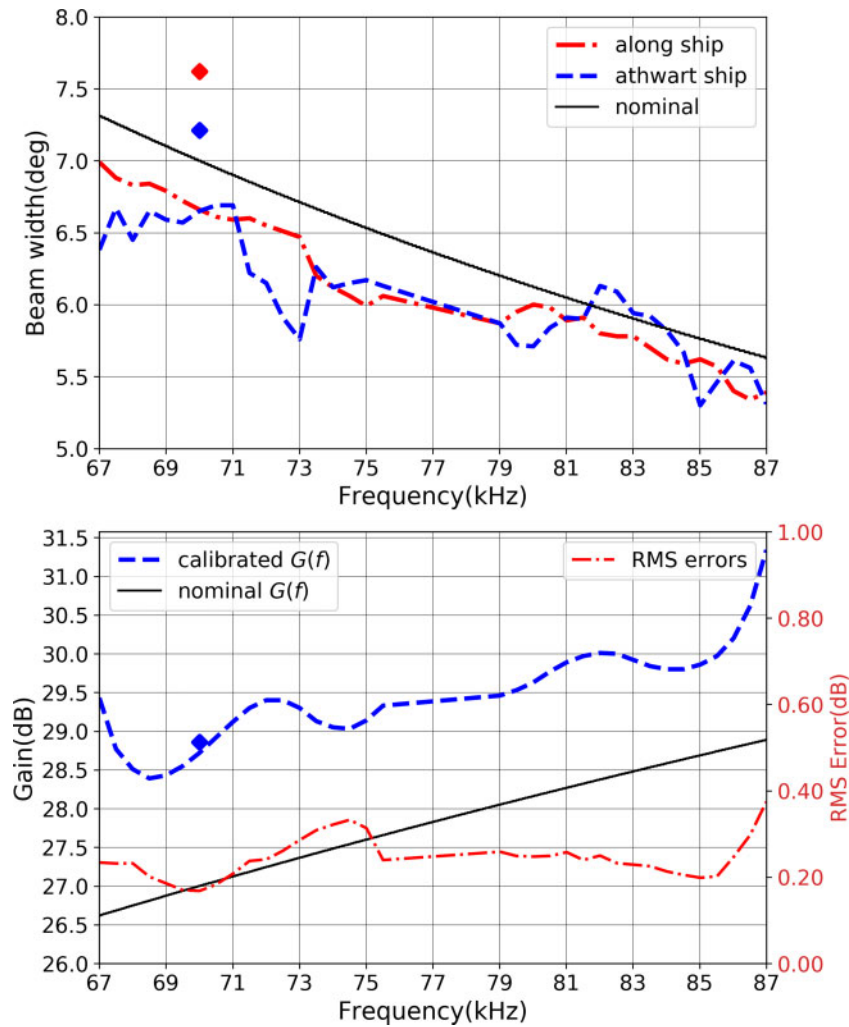


Figure 4. LFM calibration results with the transducer nominal characteristics. The top panel shows the calculated beamwidths (dashed lines) in the alongships and athwartships and the nominal (manufacturer) beamwidth (solid line), with the values obtained from the CW calibration indicated by the red and blue diamonds. The bottom panel shows the calibrated gain and RMS error (dash lines) inside the frequency band from 67 to 87 kHz and nominal (manufacturer) gain (solid line), with the value obtained from the CW calibration as the blue diamond.

manual describes procedures for how to avoid noise spikes in the working spectrum (Simrad, 2020). For the Node1 echosounder transducer, nominally from 45 to 90 kHz, the noise spectrum was observed in passive mode using the Built In Test Equipment view of the EK80 software. For the LFM calibration, the calibration sphere was moved in the same way as for the CW calibration, and measurements of the backscattering of the sphere in numerous positions across the acoustic beam were taken. In a split-beam calibration of a broadband system, the transducer gain and the beamwidths are frequency dependent. The gain as a function of frequency $G(f)$, the alongships and athwartships angles, and -3 dB beamwidths are estimated by comparing the theoretical backscattering values and the measured backscattering values for a calibration sphere. The EK80 software generates calibration results from the fitting procedure. The equations and implementation details in the EK80 software are presently in review for publishing (Andersen *et al.*, 2020). Figure 4 shows the main results from the LFM measurements of the same calibration sphere, $G(f)$ and beamwidth as a function of frequency in terms

of alongships and athwartships angles. The bottom panel of Figure 3 shows that the RMS errors are below 0.3 dB at most frequencies and the maximum RMS error is 0.37 dB at 87 kHz.

Summary

From our experience since the start of the LoVe observatory, it is not easy to calibrate the echosounder at the operating depth, due to either lack of qualifications at system manufactures, or lack of calibration demands in the initial specifications. Without retrieving the observatory, it is impossible to perform calibrations using the same method as used for vessel echosounder calibrations. For the observatory echosounder, the *in situ* calibration method suggested here is simple compared to other earlier proposed methods. The quality of the calibration can be improved by reducing the distance from transducer to the target. For any practical fishery acoustic work, the quality of the calibration is acceptable within ± 0.3 dB in both CW and LFM pulse modes, conducted at a range of 180 m from the transducer, which is adequate

measurement accuracy, corresponding to a 7% uncertainty in density measurement.

Compared to a standard vessel calibration with the target at about 20 m, the variability increases with the pulse volume at 180 m range, in which reverberating targets (zooplankton) were inside the pulse volume and some fish targets were observed between the transducer and the calibration sphere. Empirically, it is known that these factors will increase the phase variability and the variance of the calibration results. Compared to the uncalibrated echosounder system, the gain difference is 1.86 dB, overestimating density by 54% if the system is not calibrated. The Node1 transducer has been operational for several years, the first years in CW mode, and in FM mode since 2017. Yearly, large quantities of spawning cod (*Gadus morhua*) pass over the echosounder. For now, more accurate density measurements and TS measurements can be made after the calibrations. We will also try to compare the sea surface backscattering measurements to evaluate if the current calibration can be applied to the earlier data sets. Although it involved the advanced vessel, other vessels with DP systems can also perform comparable calibrations during their regular fishery surveys in the area, if the procedure for doing the calibration could be made. The measurements and calibration results prove that the method is acceptable, practical, and cost effective.

Data availability

The data in this article will be shared on request to the corresponding author.

Acknowledgements

The authors specially thank the IMR instrument chief engineer Asgeir Steinsland and the crew of R/V Kronprins Haakon. The authors also thank the Research Council of Norway for funding the Lofoten-Vesterålen cabled observatory.

References

- Andersen, L. N., Chu, D., Heimvoll, H., Korneliussen, R. J., Macaulay, G. J., and Ona, E. 2020. Quantitative processing of broadband data as implemented in a scientific splitbeam echosounder. The Journal of the Acoustical Society of America, submitted for publication.
- Andersen, L. N., Ona, E., and Macaulay, G. 2013. Measuring fish and zooplankton with a broadband split beam echo sounder. In 2013 MTS/IEEE OCEANS—Bergen, pp. 1–4.
- Andersen, L. N., Ona, E., Pedersen, G., Tichy, F., and Lunde, E. B. 2008. Measuring the equivalent beam angle of echo sounders with split-beam transducers. The Journal of the Acoustical Society of America, 123: 3436–3436.
- Barnes, C. R., Best, M. M. R., Johnson, F. R., and Pirenne, B. 2010. Final installation and initial operation of the world's first regional cabled ocean observatory (NEPTUNE Canada). Canadian Meteorological and Oceanographic Society, 38: 89–96.
- Dalen, J., Nedreaas, K., and Pedersen, R. 2003. A comparative acoustic-abundance estimation of pelagic redfish (*Sebastes mentella*) from hull-mounted and deep-towed acoustic systems. ICES Journal of Marine Science, 60: 472–479.
- Demer, D. A., Berger, L., Bernasconi, M., Bethke, E., Boswell, K., Chu, D., Domokos, R., *et al.* 2015. Calibration of acoustic instruments, pp. 49–50.
- DNVGL. 2015. DNVGL-RP-E306: Dynamic Positioning Vessel Design Philosophy Guidelines.
- Favali, P., and Beranzoli, L. 2006. Seafloor observatory science: a review. Annals of Geophysics, 49: 515–567.
- Godø, O. R., Johnsen, S., and Torkelsen, T. 2014. The LoVe ocean observatory is in operation. Marine Technology Society Journal, 48: 24–30.
- Haris, K., Kloser, R. J., Ryan, T. E., and Malan, J. 2018. Deep-water calibration of echosounders used for biomass surveys and species identification. ICES Journal of Marine Science, 75: 1117–1130.
- Jacopo, A., Damianos, C., Simone, M., Emanuela, F., Roberto, D., Sascha, F., Nadine, L., *et al.* 2019. New high-tech flexible networks for the monitoring of deep-sea ecosystems. Environmental Science & Technology, 53: 6616–6631.
- Kloser, R. J. 1996. Improved precision of acoustic surveys of benthopelagic fish by means of a deep-towed transducer. ICES Journal of Marine Science, 53: 407–413.
- Ona, E. 1990. Optimal acoustic beam pattern corrections for split beam transducers. ICES: 1990/B: 1930.
- Ona, E. 1999. Methodology for target-strength measurements. ICES Cooperative Research Report No. 235.
- Ona, E., and Barange, M. 1999. Single target recognition, ICES Cooperative Research Report 235, pp. 28–43.
- Ona, E., Mazauric, V., and Andersen, L. N. 2009. Calibration methods for two scientific multibeam systems. ICES Journal of Marine Science, 66: 1326–1334.
- Patel, R. 2006. Surveillance of Marine Resources by Use of Stationary Platforms and Autonomous Underwater Vehicle (AUV). Department of Electronics and Telecommunications, Norwegian University of Science and Technology, Trondheim.
- Patel, R., and Ona, E. 2009. Measuring herring densities with one real and several phantom research vessels. ICES Journal of Marine Science, 66: 1264–1269.
- Ryan, T. E., Kloser, R. J., and Macaulay, G. J. 2009. Measurement and visual verification of fish target strength using an acoustic-optical system attached to a trawl net. ICES Journal of Marine Science, 66: 1238–1244.
- Simmonds, J., and MacLennan, D. N. 2005. Fisheries Acoustics: Theory and Practice, Blackwell Science Ltd, Oxford, UK. 456 pp.
- Simrad. 2020. Scientific Wide Band Echo Sounder: Reference Manua https://www.simrad.online/ek80/ref_en/.
- Slotte, A., Salthaug, A., Utne, K. R., Ona, E., Vatnehol, S., and Pena, H. 2016. Distribution and Abundance of Norwegian Spring Spawning Herring during the Spawning Season in 2016. ISSN: 15036294. Institute of Marine Research.
- Smith, L., Barth, J., Kelley, D., Plueddemann, A., Rodero, I., Ulses, G., Vardaro, M., *et al.* 2018. The ocean observatories initiative. Oceanography, 31: 16–35.
- Smith, L. M., Yarincik, K., Vaccari, L., Kaplan, M. B., Barth, J. A., Cram, G. S., Fram, J. P., *et al.* 2019. Lessons learned From the United States ocean observatories initiative. Frontiers in Marine Science, 5: 1–7.
- Yang, Y., Liu, Y., Sun, D., Xu, T., Xue, S., Han, Y., and Zeng, A. 2020. Seafloor geodetic network establishment and key technologies. Science China Earth Sciences, 63, 1188–1198.

Handling editor: David Demer